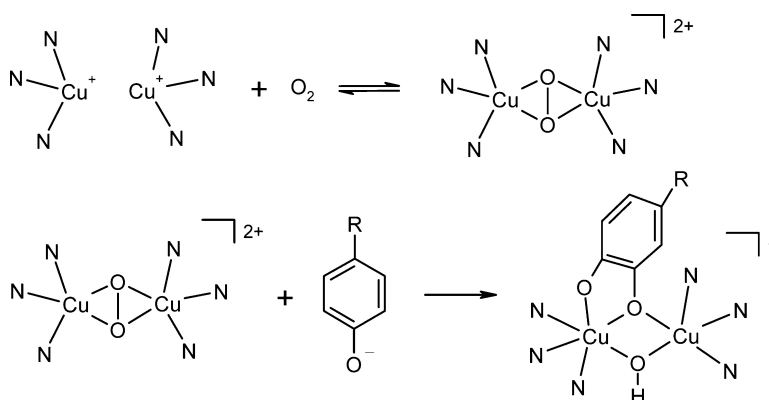


Hydroxylation of Phenolic Compounds by a Peroxodicopper(II) Complex: Further Insight into the Mechanism of Tyrosinase

Sara Palavicini, Alessandro Granata, Enrico Monzani, and Luigi Casella

J. Am. Chem. Soc., **2005**, 127 (51), 18031-18036 • DOI: 10.1021/ja0544298 • Publication Date (Web): 02 December 2005

Downloaded from <http://pubs.acs.org> on March 25, 2009



More About This Article

Additional resources and features associated with this article are available within the HTML version:

- Supporting Information
- Links to the 7 articles that cite this article, as of the time of this article download
- Access to high resolution figures
- Links to articles and content related to this article
- Copyright permission to reproduce figures and/or text from this article

[View the Full Text HTML](#)

Hydroxylation of Phenolic Compounds by a Peroxodicopper(II) Complex: Further Insight into the Mechanism of Tyrosinase

Sara Palavicini, Alessandro Granata, Enrico Monzani, and Luigi Casella*

Contribution from the Department of General Chemistry, University of Pavia,
27100 Pavia, Italy

Received July 5, 2005; Revised Manuscript Received October 28, 2005; E-mail: bioinorg@unipv.it

Abstract: The dicopper(I) complex $[\text{Cu}_2(\text{MeL66})]^{2+}$ (where MeL66 is the hexadentate ligand 3,5-bis-{2-(1-methyl-1H-benzimidazol-2-yl)-ethyl}-amino}-methylbenzene) reacts reversibly with dioxygen at low temperature to form a μ -peroxo adduct. Kinetic studies of O_2 binding carried out in acetone in the temperature range from -80 to -55 °C yielded the activation parameters $\Delta H_1^\ddagger = 40.4 \pm 2.2$ kJ mol $^{-1}$, $\Delta S_1^\ddagger = -41.4 \pm 10.8$ J K $^{-1}$ mol $^{-1}$ and $\Delta H_{-1}^\ddagger = 72.5 \pm 2.4$ kJ mol $^{-1}$, $\Delta S_{-1}^\ddagger = 46.7 \pm 11.1$ J K $^{-1}$ mol $^{-1}$ for the forward and reverse reaction, respectively, and the binding parameters of O_2 $\Delta H^\ddagger = -32.2 \pm 2.2$ kJ mol $^{-1}$ and $\Delta S^\ddagger = -88.1 \pm 10.7$ J K $^{-1}$ mol $^{-1}$. The hydroxylation of a series of *p*-substituted phenolate salts by $[\text{Cu}_2(\text{MeL66})\text{O}_2]^{2+}$ studied in acetone at -55 °C indicates that the reaction occurs with an electrophilic aromatic substitution mechanism, with a Hammett constant $\rho = -1.84$. The temperature dependence of the phenol hydroxylation was studied between -84 and -70 °C for a range of sodium *p*-cyanophenolate concentrations. The rate plots were hyperbolic and enabled to derive the activation parameters for the monophenolase reaction $\Delta H^\ddagger_{\text{ox}} = 29.1 \pm 3.0$ kJ mol $^{-1}$, $\Delta S^\ddagger_{\text{ox}} = -115 \pm 15$ J K $^{-1}$ mol $^{-1}$, and the binding parameters of the phenolate to the μ -peroxo species $\Delta H^\ddagger_{\text{b}} = -8.1 \pm 1.2$ kJ mol $^{-1}$ and $\Delta S^\ddagger_{\text{b}} = -8.9 \pm 6.2$ J K $^{-1}$ mol $^{-1}$. Thus, the complete set of kinetic and thermodynamic parameters for the two separate steps of O_2 binding and phenol hydroxylation have been obtained for $[\text{Cu}_2(\text{MeL66})]^{2+}$.

Introduction

The biomimetic chemistry of copper proteins and enzymes that bind dioxygen and/or promote oxidative processes has produced a variety of synthetic systems that contributed to our understanding of how proteins function.^{1,2} The active site pattern shown by copper oxidases and oxygenases is very broad, as it includes sites with one, two, three, or four metal ions.³ But the majority of biomimetic studies have been inspired so far by the dicopper unit present in hemocyanin,⁴ tyrosinase,⁵ and catechol oxidase,⁶ where three histidines are bound to each metal center. Despite the structural similarity, the three types of proteins exhibit different reactivity: hemocyanin is a dioxygen carrier, tyrosinase a monooxygenase and catechol oxidase a simple oxidase.³ While the oxidation of catechols is relatively easy to reproduce in copper model systems,⁷ only a few genuine tyrosinase models have been reported, in which a μ - η^2 : η^2 -peroxodicopper(II) complex hydroxylates an exogenous phe-

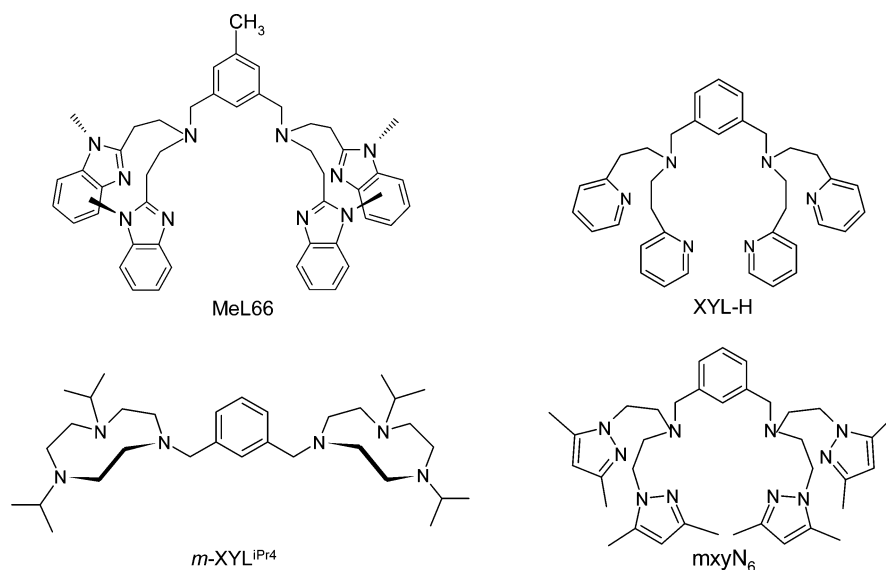
nolate to yield the corresponding catechol or quinone derivative.^{8–11} Our first report of such a reaction⁸ described a system in which the peroxo complex is generated within a dinuclear complex, with the ligand (L66) providing six nitrogen donors, whereas in the other cases the peroxo complex results from the association of two mononuclear units.^{9–11} The nature of electrophilic aromatic substitution of the phenol hydroxylation has been clarified by Itoh and co-workers on a series of *p*-substituted phenolic substrates.^{9,12} We report here further mechanistic insight into the monophenolase reaction using the μ - η^2 : η^2 -peroxodicopper(II) complex derived from the ligand 3,5-bis-{bis-[2-(1-methyl-1H-benzimidazol-2-yl)-ethyl]-amino}-methylbenzene (MeL66), analogous to the previously studied L66 but carrying a methyl substituent on the xylyl ring (Chart 1). The increased solubility of the Cu^{I} complex of MeL66 with respect to L66 at low-temperature allowed to carry out a complete study of the Cu^{I} oxygenation and phenol hydroxylation reactions at variable temperatures (Scheme 1), yielding activation and thermodynamic parameters controlling the two steps of the monophenolase reaction.

* Dipartimento di Chimia Generale, Via Taramelli 12, 27100 Pavia, Italy.

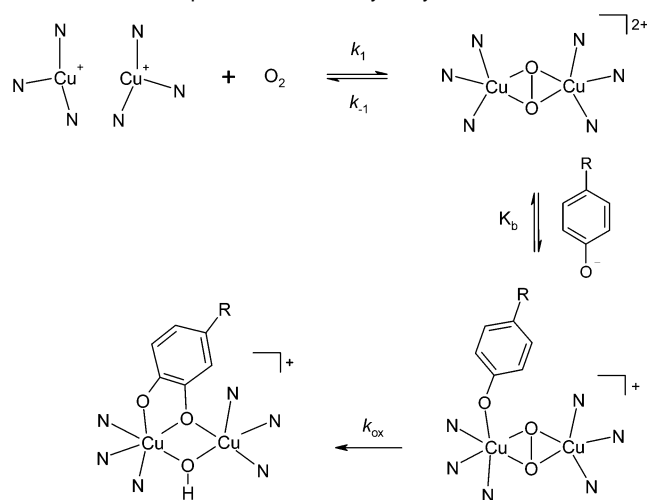
- (1) Lewis, E. A.; Tolman, W. B. *Chem. Rev.* **2004**, *104*, 1047–1076.
- (2) Hatcher, L. Q.; Karlin, K. D. *J. Biol. Inorg. Chem.* **2004**, *9*, 66–683.
- (3) Solomon, E. I.; Sundaram, U. M.; Machonkin, T. E. *Chem. Rev.* **1996**, *96*, 2563–2605.
- (4) Cuff, M. E.; Miller, C.; van Holde, K. E.; Hendrickson, W. A. *J. Mol. Biol.* **2000**, *278*, 855–870.
- (5) Land, E. J.; Ramsden, C. A.; Riley P. A. *Acc. Chem. Res.* **2003**, *36*, 300–308.
- (6) Gerdemann, C.; Eicken, C.; Krebs, B. *Acc. Chem. Res.* **2002**, *35*, 183–191.
- (7) Battaini, G.; Granata, A.; Monzani, E.; Gullotti, M.; Casella, L. *Adv. Inorg. Chem.*, in press.

- (8) Santagostini, L.; Gullotti, M.; Monzani, E.; Casella, L.; Dillinger, R.; Tuzcek, F. *Chem.–Eur. J.* **2000**, *6*, 519–522.
- (9) Itoh, S.; Kumei, H.; Taki, M.; Nagatomo, S.; Kitagawa, T.; Fukuzumi, S. *J. Am. Chem. Soc.* **2001**, *123*, 6708–6709.
- (10) Mirica, L. M.; Vance, M.; Rudd, D. J.; Hedman, B.; Hodgson, K. O.; Solomon, E. I.; Stack, T. D. P. *J. Am. Chem. Soc.* **2002**, *124*, 9332–9333.
- (11) Battaini, G.; De Carolis, M.; Monzani, E.; Tuzcek, F.; Casella, L. *Chem. Commun.* **2003**, 726–727.
- (12) Yamazaki, S.-I.; Itoh, S. *J. Am. Chem. Soc.* **2003**, *125*, 13034–13035.

Chart 1



Scheme 1 Two Steps of the Phenol Hydroxylation Reaction



Experimental Section

General Procedures. All reagents were purchased from commercial sources and used as received unless otherwise noted. DMF and dichloromethane were freshly distilled over CaH₂, acetone was dried by distillation over CaSO₄. *N,N'*-Bis[2-(1'-methyl-2'-benzimidazolyl)ethyl]amine was prepared as described previously.¹³ Infrared spectra were recorded on a Perkin-Elmer Spectrum BX FT/IR instrument. NMR spectra were recorded on a Bruker AVANCE 400 spectrometer. Optical spectra were measured on HP 8452A and 8453 diode array spectrophotometers. The low-temperature spectra and kinetics were performed with a custom designed immersible fiber-optic quartz probe (HELLMA) fitted to a Schlenk vessel and connected with the diode array spectrophotometer.

Synthesis of the Ligand MeL66. The ligand MeL66 was prepared following a procedure similar to that described before for L66.¹³ *N,N'*-Bis[2-(1'-methyl-2'-benzimidazolyl)ethyl]amine (3.82 g, 11.5 mmol), dry Na₂CO₃ (0.24 g, 2.25 mmol), and 1,3-bis(bromomethyl)-5-methylbenzene (0.25 g, 0.90 mmol) were

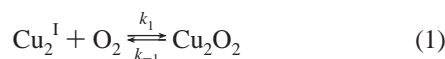
reacted at 85 °C under stirring for 55 h in dry DMF (freshly distilled over CaH₂) (50 mL) under an inert atmosphere. After cooling to room temperature, a precipitate was obtained by addition of cold water. The crude MeL66 product was purified by column chromatography on silica (4 × 40 cm), using an eluent mixture of CH₂Cl₂/MeOH 15:1 containing 1% NEt₃ (v/v). Anal. Calcd for C₄₉H₅₄N₁₀·4H₂O: C, 68.83; H, 7.31; N, 16.38. Found: C, 69.20; H, 7.43; N, 16.55. ¹H NMR (400 MHz, CDCl₃, 20 °C, TMS): δ 7.68 (m, 4H; benzimidazole-H), 7.20–7.24 (m, 12H; benzimidazole-H), 6.94 (s, 1H; phenyl-H), 6.92 (s, 2H; phenyl-H), 3.66 (s, 4H; N-CH₂-phenyl), 3.52 (s, 12H; N-CH₃), 3.13 (t, ³J(H,H) = 7.8 Hz, 8H; N-CH₂-CH₂-benzimidazole), 2.99 (t, ³J(H,H) = 7.8 Hz, 8H; N-CH₂-CH₂-benzimidazole), 2.14 (s, 3H; CH₃-phenyl).

Synthesis of Complex [Cu₂(MeL66)](PF₆)₂. To a solution of the ligand MeL66 (0.040 g, 0.051 mmol) in dry CH₂Cl₂ (20 mL) kept under an inert atmosphere, solid [Cu(CH₃CN)₄](PF₆) (0.032 g, 0.102 mmol) was added under stirring. Stirring was continued for about 15 min, and then the mixture was concentrated under vacuum. The precipitate of Cu^I complex was collected by filtration under an inert atmosphere, washed with a small amount of degassed CH₂Cl₂, and carefully dried under vacuum (yield 50%). Anal. Calcd for Cu₂C₄₉H₅₄N₁₀·2CH₂Cl₂: 44.57; H, 4.22; N, 10.20. Found: C, 44.93; H, 4.61; N, 10.68. ¹H NMR (400 MHz, CD₃COCD₃, -80 °C, TMS): δ 7.22–7.60 (m, 16H; benzimidazole-H), 7.20 (s, 1H; phenyl-H), 6.81 (s, 2H; phenyl-H), 4.44 (s, 4H; N-CH₂-phenyl), 3.70 (12H; N-CH₃), 3.14 (m, 8H; N-CH₂-CH₂-benzimidazole), 3.04 (broad, 8H; N-CH₂-CH₂-benzimidazole), 2.15 (s, 3H; CH₃-phenyl).

Kinetics of O₂ Binding to [Cu₂(MeL66)]²⁺. The kinetics of O₂ binding to [Cu₂(MeL66)]²⁺ were studied at 362 nm, in the range from -80 to -55 °C, upon injecting a small volume of a chilled concentrated solution of the Cu^I complex into O₂-saturated acetone (25 mL) thermostated at the appropriate temperature (final concentration of the complex 3 × 10⁻⁵ M). The growth of the absorption band of the peroxo complex follows an exponential behavior, with a rate constant k_{obs} . The value of k_{obs} was obtained at each temperature from a fitting of the absorbance data vs time. The process can be accounted for

(13) Casella, L.; Gullotti, M.; Radaelli, R.; Di Gennaro, P. *J. Chem. Soc. Chem. Commun.* **1991**, 1611–1612.

by the reversible oxygenation equilibrium 1



The rate equation can be obtained solving the differential equation for the formation of the Cu_2O_2 complex vs time, together with the mass balance on copper. By consideration that dioxygen is in strong excess (so that its consumption can be neglected) and that at zero time the complex is completely in the copper(I) form, the formation of the Cu_2O_2 complex vs time can be described with the following eq 2⁸

$$[\text{Cu}_2\text{O}_2] = \frac{k_1[\text{O}_2][\text{Cu}_2^{\text{I}}]_0}{k_1[\text{O}_2] + k_{-1}} \{1 - \exp[-(k_1[\text{O}_2] + k_{-1}) \times t]\} \quad (2)$$

where $[\text{Cu}_2^{\text{I}}]_0$ is the initial concentration of $[\text{Cu}_2(\text{MeL66})]^{2+}$. Thus, the observed rate constant k_{obs} is an ensemble of constants depending on both the forward and backward processes

$$k_{\text{obs}} = k_1[\text{O}_2] + k_{-1} \quad (3)$$

The rate constant k_{-1} was obtained from the first-order spectral changes at 362 nm occurring upon applying a vacuum to the oxygenated (1 atm) solution of $[\text{Cu}_2(\text{MeL66})]^{2+}$ at the appropriate temperature. The solubility of dioxygen in acetone at low temperature was taken from the literature¹⁴ and was always much larger than the initial concentration of $[\text{Cu}_2(\text{MeL66})]^{2+}$. The stoichiometry of dioxygen binding to $[\text{Cu}_2(\text{MeL66})]^{2+}$ was determined through the amount of hydrogen peroxide produced by addition of excess trifluoroacetic acid to the oxygenated solution at -80°C , according to the previously described peroxidase/ABTS assay.⁸ The yield of hydrogen peroxide found considering a $2\text{Cu}:1\text{O}_2$ stoichiometry was about 98%.

Hydroxylation of *p*-Carbomethoxyphenolate. The peroxo complex $[\text{Cu}_2(\text{MeL66})\text{O}_2](\text{PF}_6)_2$ was generated by the reaction of $[\text{Cu}_2(\text{MeL66})](\text{PF}_6)_2$ (8.25×10^{-4} mmol) and O_2 (1 atm) at -55°C in anhydrous acetone (25 mL) for 20 min. The amount of peroxo complex formed in these conditions was 88%, with respect to the initial Cu(I) complex, as it has been confirmed in a separate experiment with the peroxidase/ H_2O_2 /ABTS assay.⁸ A cooled solution of sodium *p*-carbomethoxyphenolate (4.95×10^{-3} mmol) in dry acetone (1 mL) was then added by a syringe. After 0.5 h, the reaction mixture was quenched by the addition of HClO_4 (0.4 M, 3 mL), and the solvent was removed until the residual volume was about 3 mL. The residue was treated with CH_2Cl_2 (20 mL), and the organic phase was washed three times with a small amount of aqueous HClO_4 and with water, and then it was taken to dryness. NMR analysis of the product mixture confirms that the only product is the catechol (methyl 3,4-dihydroxybenzoate)¹⁵ in >90% yield with respect to $[\text{Cu}_2(\text{MeL66})\text{O}_2]^{2+}$.

Kinetics of the Reactions of $[\text{Cu}_2(\text{MeL66})\text{O}_2](\text{PF}_6)_2$ with Phenolates. The peroxo complex $[\text{Cu}_2(\text{MeL66})\text{O}_2](\text{PF}_6)_2$ was generated by the reaction of $[\text{Cu}_2(\text{MeL66})](\text{PF}_6)_2$ (8.25×10^{-4} mmol) and O_2 in anhydrous acetone (25 mL) at the desired

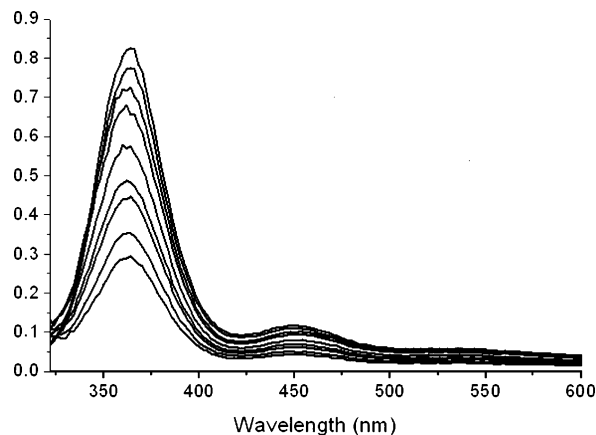


Figure 1. Selected difference UV-vis spectra recorded at different times during the oxygenation of $[\text{Cu}_2(\text{MeL66})]^{2+}$ (0.11 mM) at -78°C in acetone solution. The reaction is complete in about 8 min.

temperature (from -55 to -84°C) until the spectral changes at 362 nm were negligible; usually 20 min were enough at -55°C while 90 min were necessary at the lowest temperature. The reactions were then initiated by the addition of pre-chilled, concentrated solutions of the phenolates, at least 5 molar equiv with respect to the peroxo complex. The reactions were followed by monitoring the disappearance of the band at 362 nm. The $A_{362\text{ nm}}$ vs time traces were fitted with a first-order equation, which allowed us to obtain the k_{obs} (s^{-1}) values. The molar ratios of $\text{R-Ph-O}^-/[\text{Cu}_2(\text{MeL66})]^{2+}$ studied for the series of *p*-substituted phenols were as follows: (a) with $\text{F-Ph-O}^- = 5-10$, (b) with $\text{Cl-Ph-O}^- = 5-15$; (c) with $\text{CH}_3\text{OOC-Ph-O}^- = 5-40$; (d) with NC-Ph-O^- (at -55°C) = 5-25; (e) with NC-Ph-O^- (at -70 , -75 , -80 , and -84°C) = 20-400.

Results and Discussion

Oxygenation of $[\text{Cu}_2(\text{MeL66})]^{2+}$. The oxygenation of $[\text{Cu}_2(\text{MeL66})]^{2+}$ in dry acetone at -78°C (Figure 1) produces a peroxo complex $[\text{Cu}_2(\text{MeL66})\text{O}_2]^{2+}$ exhibiting an electronic spectrum with ligand-metal charge-transfer (LMCT) features (λ_{max} 362 nm, ϵ 15 400 $\text{M}^{-1}\text{cm}^{-1}$, and 454 nm, ϵ 2 800 $\text{M}^{-1}\text{cm}^{-1}$) practically identical with those of the parent $[\text{Cu}_2(\text{L66})\text{O}_2]^{2+}$ system.⁸ These peroxo complexes, of $^{\text{S}}\text{P}$ type in the Stack classification,¹⁶ likely contain a “butterfly” bending of the Cu_2O_2 core,¹⁷ as suggested by the presence of the low-intensity LMCT component near 450 nm. The oxygenation occurs in a single observable step and is fully reversed by application of a vacuum (see Supporting Information). The process of O_2 binding and release was studied at various temperatures and the corresponding rate constants, k_1 and k_{-1} (Scheme 1), were determined. From these values, the activation parameters for the forward and reverse oxygenation reaction and the binding parameters of O_2 were derived (Table 1). Also included in Table 1 are values of the equilibrium constants ($K_{\text{eq}} = k_1/k_{-1}$) calculated at selected temperatures.

It is useful to compare these data with those obtained, in the same solvent, for dioxygen binding to the Cu^{I}_2 complexes more closely related to $[\text{Cu}_2(\text{MeL66})]^{2+}$, i.e., those derived from the

(14) Mahapatra, S.; Kaderli, S.; Llobet, A.; Neuhold, Y.-M.; Palanchè, T.; Halfen, J. A.; Young, V. G., Jr.; Kaden, T. A.; Que, L., Jr.; Zuberbühler, A. D.; Tolman, W. B. *Inorg. Chem.* **1997**, *36*, 6343–6356.
 (15) Casella, L.; Monzani, E.; Gullotti, M.; Cavagnino, D.; Cerina, G.; Santagostini, L.; Ugo, R. *Inorg. Chem.* **1996**, *35*, 7516–7525.

(16) Mirica, L. M.; Ottenwaelder, X.; Stack, T. D. P. *Chem. Rev.* **2004**, *104*, 1013–1045.

(17) Pidcock, E.; Obias, H. V.; Abe, M.; Liang, H. C.; Karlin, K. D.; Solomon, E. I. *J. Am. Chem. Soc.* **1999**, *121*, 1299–1308.

Table 1. Kinetic and Thermodynamic Parameters for the Formation of Peroxo Complexes upon Low Temperature Oxygenation of Dinuclear Copper(I) Complexes in Acetone Solution

complexes	activation parameters (from k_1) ^a	activation parameters (from k_{-1}) ^a	thermodynamic parameters (from K_{eq}) ^a	K_{eq} (TK) ^b	refs
MeL66	$\Delta H_1^\ddagger = 40.4 \pm 2.2$ $\Delta S_1^\ddagger = -41.4 \pm 10.8$	$\Delta H_{-1}^\ddagger = 72.5 \pm 2.4$ $\Delta S_{-1}^\ddagger = 46.7 \pm 11.1$	$\Delta H^\circ = -32.2 \pm 2.2$ $\Delta S^\circ = -88.1 \pm 10.7$	1.2×10^4 (195) 2.5×10^3 (210)	this work
XYL-H	$\Delta H_1^\ddagger = 2.1 \pm 0.7$ $\Delta S_1^\ddagger = -174 \pm 3$	$\Delta H_{-1}^\ddagger = 80.3 \pm 0.8$ $\Delta S_{-1}^\ddagger = 77 \pm 3$	$\Delta H^\circ = -42.3 \pm 0.4$ $\Delta S^\circ = -176 \pm 2$	2.7×10^6 (193) ^c 1.7×10^4 (223) ^d	19,20
<i>m</i> -XYL ^{iPr4}	$\Delta H_1^\ddagger = 39.4 \pm 0.5$ $\Delta S_1^\ddagger = -30 \pm 2$				14

^a Units are kJ mol⁻¹ (ΔH^\ddagger or ΔH°) or J K⁻¹ mol⁻¹ (ΔS^\ddagger or ΔS°). ^b Units are M⁻¹. ^c K_{eq} value in CH₂Cl₂ solution (see Cruse, R. W.; Kaderli, S.; Karlin, K. D.; Zuberbühler, A. D. *J. Am. Chem. Soc.* **1988**, *110*, 6882–6883). ^d In CH₂Cl₂ solution, see ref 26.

dinucleating ligands XYL-H and *m*-XYL^{iPr4} (Chart 1). For both these complexes the dioxygen adducts are of **SP** type,¹⁶ at least in dilute solution in the case of [Cu₂(*m*-XYL^{iPr4})²⁺],¹⁴ but the oxygenation behavior is quite different in the two cases. For [Cu₂(*m*-XYL^{iPr4})²⁺], the rate-limiting step of the reaction with O₂ is formation of the 1:1 Cu–O₂ complex, which evolves through intra- or intermolecular pathways to generate μ -peroxo or bis- μ -oxo Cu₂O₂ cores.^{1,14} In the case of [Cu₂(XYL-H)]²⁺, the oxygenation proceeds to the peroxo species without any observable 1:1 Cu–O₂ species.^{18–20} As shown by the data collected in Table 1, the activation parameters connected with the formation of the 1:1 CuO₂ complex in Tolman's [Cu₂(*m*-XYL^{iPr4})²⁺] system are indeed similar to those found here, while a small activation enthalpy and a large negative activation entropy occur with Karlin's [Cu₂(XYL-H)]²⁺ system.^{18–20} Even though we cannot exclude that the oxygenation of [Cu₂(MeL66)]²⁺ follows a pathway similar to that of [Cu₂(*m*-XYL^{iPr4})²⁺], we think that the behavior of [Cu₂(MeL66)]²⁺ corresponds to that of [Cu₂(XYL-H)]²⁺, due to the strong similarity in donor properties of the heterocyclic benzimidazole and pyridine groups in the sidearms of the MeL66 and XYL-H ligands. The soft heterocyclic nitrogen donors and the flexible six-membered chelate rings occurring in these complexes are likely to assist the Cu^I–O₂ interaction much more than the hard, aliphatic 1,4,7-triazacyclononane moieties, forming smaller five-membered chelate rings, in [Cu₂(*m*-XYL^{iPr4})²⁺].^{14,16} The difference in activation parameters between the MeL66 and XYL-H systems could be thus ascribed to the role played by the four aromatic substituents in the conformational changes undergone by the Cu₂ complex on μ -peroxo adduct formation. The larger enthalpy barrier for O₂ binding to [Cu₂(MeL66)]²⁺ with respect to [Cu₂(XYL-H)]²⁺ is probably contributed by two factors: (i) the slower conformational rearrangement of the bulkier *N*-methyl-benzimidazole vs the pyridine groups and (ii) the loss of favorable aromatic ring stacking interactions occurring in the Cu₂ complex. The structure of [Cu₂(MeL66)]²⁺, rather than that of [Cu₂(XYL-H)]²⁺,²¹ most likely resembles that of [Cu₂(mxyN₆)]²⁺,²² where dimethylpyrazoles replace the pyridine moieties in the sidearms of the ligand (Scheme 1). In [Cu₂(mxyN₆)]²⁺, the Cu^{••}–Cu distance (5.1 Å) is much shorter than in [Cu₂(XYL-H)]²⁺ (8.9 Å) and the folded conformation of the ligand is apparently maintained by ring stacking interactions between dimethylpyrazole rings.²² The similar five-membered-

ring size of the *N*-heterocycles pyrazole and benzimidazole and the more extended aromatic character of benzimidazoles suggest that the same structural arrangement should be present in [Cu₂(MeL66)]²⁺. Upon formation of the μ -peroxo complex [Cu₂(MeL66)O₂]²⁺ the ring-stacking interaction is probably lost or strongly weakened because the *N*-methyl-benzimidazoles move at larger distances. The loss in the ring stacking interaction appears to be supported by the activation entropy parameter for O₂ binding, which is significantly less negative for the MeL66 than for the XYL-H system, in agreement with some increase in the conformational mobility of the ligand.

The equilibrium constants for the oxygenation of [Cu₂(XYL-H)]²⁺ reported in Table 1 refer to dichloromethane solution, because corresponding data at low temperature in acetone solution are not available.²⁰ However, both the activation and thermodynamic parameters are similar in the two solvents,^{20,23,26} and this makes the comparison between the K_{eq} values for O₂ binding to [Cu₂(XYL-H)]²⁺ and [Cu₂(MeL66)]²⁺ in the same temperature range feasible. Overall, the [Cu₂(XYL-H)O₂]²⁺ complex is significantly more stable than [Cu₂(MeL66)O₂]²⁺; a similar conclusion was reached previously with [Cu₂(L66)O₂]²⁺ on the basis of the equilibrium data at –78 °C.⁸ In particular, the O₂ binding parameters highlight a peroxodicopper(II) bond intrinsically weaker in [Cu₂(MeL66)O₂]²⁺ (–32.2 ± 2.2 kJ mol⁻¹) compared to [Cu₂(XYL-H)O₂]²⁺ (–42.3 ± 0.4 kJ mol⁻¹),^{19,20} probably because some steric interaction between the *N*-methyl-benzimidazole groups prevents an optimal approach of the two copper atoms in the Cu₂O₂ core. Some strain in Cu₂–O₂ bonding is inherent in the systems where the ligand contains xylyl groups connecting two tridentate donor units. This is shown by the considerably more negative ΔH° values (less than –80 kJ mol⁻¹) for dioxygen binding to the dinuclear Cu^I complexes with the Nn ligands containing two bis(pyridylethyl)amine arms as in [Cu₂(XYL-H)]²⁺ but connected by much more flexible polymethylene linkers in the place of the *m*-xylyl group.²³

Another important aspect in which the MeL66 and mxyN₆ systems differ with respect to the XYL-H and *m*-XYL^{iPr4} systems is the thermal decay of the Cu₂O₂ species, or the direct reaction between the Cu₂ complexes and dioxygen at room temperature. In the XYL-H and *m*-XYL^{iPr4} systems; in fact, the Cu₂O₂ species give an intramolecular electrophilic attack on the

- (18) Karlin, K. D.; Nasir, M. S.; Cohen, B. I.; Cruse, R. W.; Kaderli, S.; Zuberbühler, A. D. *J. Am. Chem. Soc.* **1994**, *116*, 1324–1336.
 (19) Karlin, K. D.; Zuberbühler, A. D. In *Bioinorganic Catalysis*, 2nd ed.; Reedijk, J., Bouwman, E., Eds.; Marcel Dekker: New York, 1999; pp 469–534.
 (20) Becker, M.; Schindler, S.; Karlin, K. D.; Kaden, T. A.; Kaderli, S.; Palanché, T.; Zuberbühler, A. D. *Inorg. Chem.* **1999**, *38*, 1989–1995.
 (21) Karlin, K. D.; Gultneh, Y.; Hutchinson, J. P.; Zubieta, J. *J. Am. Chem. Soc.* **1982**, *104*, 5240–5242.

- (22) Sorrell, T. N.; Malachowski, M. R.; Jameson, D. L. *Inorg. Chem.* **1982**, *21*, 3250–3252.
 (23) Liang, H.-C.; Karlin, K. D.; Dyson, R.; Kaderli, S.; Jung, B.; Zuberbühler, A. D. *Inorg. Chem.* **2000**, *39*, 5884–5894.
 (24) Karlin, K. D.; Gultneh, Y.; Hayes, J. C.; Cruse, R. W.; McKown, J. W.; Hutchinson, J. P.; Zubieta, J. *J. Am. Chem. Soc.* **1984**, *106*, 2121–2128.
 (25) Nasir, M. S.; Cohen, B. I.; Karlin, K. D. *J. Am. Chem. Soc.* **1992**, *114*, 2482–2494.
 (26) Karlin, K. D.; Nasir, M. S.; Cohen, B. I.; Cruse, R. W.; Kaderli, S.; Zuberbühler, A. D. *J. Am. Chem. Soc.* **1994**, *116*, 1324–1336.

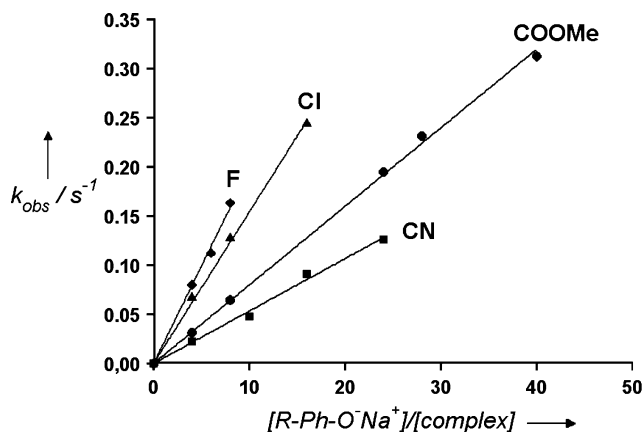
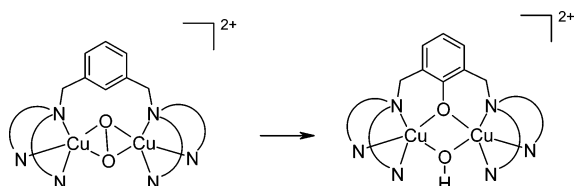


Figure 2. Plots of k_{obs} vs molar ratio of $\text{R-Ph-O}^-/[\text{Cu}_2(\text{MeL66})\text{O}_2]^{2+}$ for a series of p -substituted phenols in acetone at $-55\text{ }^\circ\text{C}$.

Scheme 2 Xylyl Ligand Hydroxylation Reaction undergone by the Cu_2O_2 Complexes Derived from XYL-H and $m\text{-XYL}^{\text{IPr}^4}$



xylyl aromatic ring, producing the corresponding μ -phenoxo- μ -hydroxo-dicopper(II) complexes (in dilute solution in the case of $m\text{-XYL}^{\text{IPr}^4}$), as shown in Scheme 2.^{14,24,25} This reaction mimics the monooxygenase activity of tyrosinase and has been studied in detail also with a variety of substituted R-XYL-H systems.^{19,26} In contrast, oxygenation at room temperature of the Cu_2 complexes of MeL66, mxyN_6 , and all other xylyl-linked dinucleating ligands containing five-membered N -heterocycles in the sidearms yields products resulting from four-electron reduction of O_2 , e.g. bis(hydroxo)dicopper(II) complexes.^{22,27,28}

Phenol Hydroxylations by $[\text{Cu}_2(\text{MeL66})\text{O}_2]^{2+}$. The phenol hydroxylation by the peroxo complex $[\text{Cu}_2(\text{MeL66})\text{O}_2]^{2+}$ was studied using the sodium salts of a series of p -substituted phenols ($p\text{-R-C}_6\text{H}_4\text{-OH}$). Comparative reactions were studied in acetone at $-55\text{ }^\circ\text{C}$, because at lower temperatures the rates were slow for phenols carrying electron-withdrawing substituents. Note that at $-55\text{ }^\circ\text{C}$ a minor fraction of the complex remains in the $[\text{Cu}_2(\text{MeL66})]^{2+}$ form, i.e., the equilibrium of peroxo complex formation is not completely shifted to the right ($K_{\text{eq}} = 1.4 \times 10^3\text{ M}^{-1}$ at $-55\text{ }^\circ\text{C}$). As the Cu^{I} oxygenation process is slower than phenolate hydroxylation, the minor fraction of complex in the reduced form had negligible effect on the rate constants obtained. The reactions followed pseudo-first-order kinetics. From the linear plots of observed kinetic constants against phenolate concentration (Figure 2), the following second-order rate constants (k_{R}) were obtained: for $\text{R}=\text{F}$, $k_{\text{F}} = 0.078\text{ M}^{-1}\text{ s}^{-1}$; for $\text{R}=\text{Cl}$, $k_{\text{Cl}} = 0.062\text{ M}^{-1}\text{ s}^{-1}$; for $\text{R}=\text{COOMe}$, $k_{\text{COOMe}} = 0.032\text{ M}^{-1}\text{ s}^{-1}$; for $\text{R}=\text{CN}$, $k_{\text{CN}} = 0.020\text{ M}^{-1}\text{ s}^{-1}$.

The plot of the rate constants for the phenol hydroxylation against the corresponding Hammett substituent constants σ^{+29}

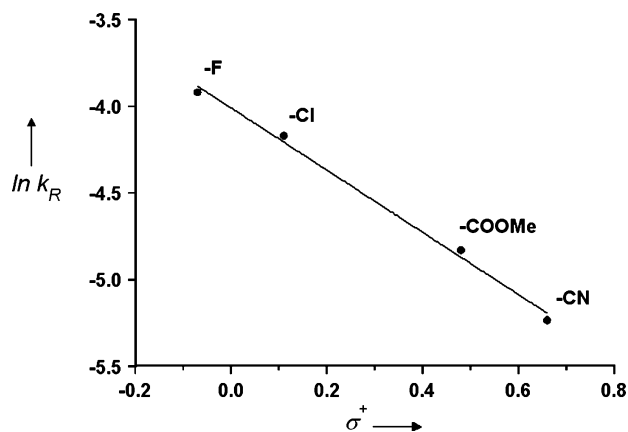


Figure 3. Hammett plot for the hydroxylation of p -substituted phenols by $[\text{Cu}_2(\text{MeL66})\text{O}_2]^{2+}$.

was linear ($R^2 = 0.99$, see Figure 3) and yielded a reaction constant $\rho = -1.84$, which is coincident with that obtained by Itoh and co-workers for their tyrosinase model system (-1.8) and close to that found for tyrosinase ($\rho = -2.4$)¹² and also for the ligand hydroxylation by $[\text{Cu}_2(\text{XYL-H})\text{O}_2]^{2+}/\text{O}_2$ ($\rho = -2.1$),¹⁹ confirming the identity of the mechanism involved. From a small-scale reaction between $[\text{Cu}_2(\text{MeL66})\text{O}_2]^{2+}$ and 6 equiv of p -carbomethoxyphenolate at $-55\text{ }^\circ\text{C}$, the catechol was isolated in $>90\%$ yield with respect to $[\text{Cu}_2(\text{MeL66})\text{O}_2]^{2+}$, with no detectable quinone, C–C or C–O phenol coupling dimers.³⁰ As shown in a previous study,¹⁵ formation of the C–O coupling dimers (formally resulting from one catechol and one phenol molecule) occurs when the phenol hydroxylation is carried out at room temperature but is not observed at low temperature. This has been confirmed in the reactions promoted by other μ -peroxodicopper(II) systems.^{9–11} On the other hand, phenol C–C dimers are formed by coupling of phenoxy radicals, which are generated through proton-coupled electron transfer from neutral phenols by the Cu_2O_2 species.³¹ This type of radical chemistry is apparently avoided by all genuine tyrosinase model systems,^{8–12} as it is in tyrosinase reactions,³² that likely function through direct oxygen transfer from the Cu_2O_2 species to the phenolate.

The hydroxylation rates were studied also for large $\text{R-Ph-O}^-/[\text{Cu}_2(\text{MeL66})\text{O}_2]^{2+}$ molar ratios. With electron-rich phenols the reactions were too fast to give reliable data even at low temperature, but rate data could be obtained with phenols carrying electron-withdrawing substituents. The rate plots become hyperbolic and reach a limiting value at high substrate concentration. This shows that the monophenolase reaction is subject to pre-equilibrium binding of the phenolate to the peroxo complex, as it has been observed previously in the reactions of Itoh's model system.⁹ The substrate dependence of the rate of phenol hydroxylation could be investigated with p -cyanophenolate over a range of temperatures, although the analysis had to be limited to the relatively narrow range between -84 and $-70\text{ }^\circ\text{C}$, because at higher temperatures the rates became too fast to be determined accurately for large phenolate concentrations. The plots were well behaved (Figure 4) and the curves were fitted to the equation: $k_{\text{obs}} = k_{\text{ox}} \times [p\text{-NC-PhO}^-]/(1/K_{\text{b}} +$

(27) Sorrell, T. N.; Vankai, V. A.; Garrity, M. L. *Inorg. Chem.* **1991**, *30*, 207–210.

(28) Casella, L.; Carugo, O.; Gullotti, M.; Garofani, S.; Zanello, P. *Inorg. Chem.* **1993**, *32*, 2056–2067.

(29) Smith, M. B.; March, J. *March's Advanced Organic Chemistry*, 5th ed.; Wiley: New York, 2001; Chapter 9.

(30) Sayre, L. M.; Nadkarni, D. V. *J. Am. Chem. Soc.* **1994**, *116*, 3157–3158.

(31) Osako, T.; Ohkubo, K.; Taki, M.; Tachi, Y.; Fukuzumi, S.; Itoh, S. *J. Am. Chem. Soc.* **2003**, *125*, 11027–11033.

(32) Ferrari, R. P.; Laurenti, E.; Ghibaudi, E. M.; Casella, L. *J. Inorg. Biochem.* **1997**, *68*, 61–69.

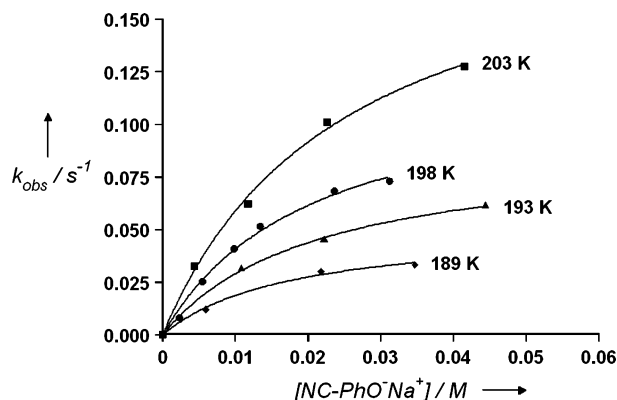


Figure 4. Temperature dependence of the rate of hydroxylation of sodium *p*-cyanophenolate by $[\text{Cu}_2(\text{MeL66})\text{O}_2]^{2+}$ studied for a range of substrate concentrations.

$[\text{p-NC-PhO}^-]$, where k_{obs} is the observed rate constant, k_{ox} the hydroxylation rate constant, and K_{b} the association constant between the phenolate and the peroxo complex.

The temperature dependence of k_{ox} yielded the activation parameters associated with the monophenolase reaction, $\Delta H^{\ddagger}_{\text{ox}} = 29.1 \pm 3.0 \text{ kJ mol}^{-1}$ and $\Delta S^{\ddagger}_{\text{ox}} = -115 \pm 15 \text{ J K}^{-1} \text{ mol}^{-1}$. The enthalpic activation barrier is significantly lower than for the intramolecular aromatic hydroxylation undergone by the XYL-H^{18,19} and *m*-XYL^{iPr4}¹⁴ ligands (Scheme 2) (50 kJ mol^{-1} in both cases), probably for the larger electron density present in the exogenous phenolate with respect to the xylyl aromatic ring, while the (negative) entropy term is much larger here than for the ligand hydroxylations ($-35 \text{ J K}^{-1} \text{ mol}^{-1}$ for the XYL-H system, $-50.4 \text{ J K}^{-1} \text{ mol}^{-1}$ for the *m*-XYL^{iPr4} system), quite certainly due to immobilization of the copper-bound phenolate in the transition state. In addition, from the temperature dependence of K_{b} , through the van't Hoff equation, the enthalpy and entropy contributions for phenolate binding to the peroxo species, $\Delta H^{\circ}_{\text{b}} = -8.1 \pm 1.2 \text{ kJ mol}^{-1}$ and $\Delta S^{\circ}_{\text{b}} = -8.9 \pm 6.2 \text{ J K}^{-1} \text{ mol}^{-1}$, respectively, were derived. Note that the binding parameters are not affected by ion pair formation in the organic solvent, since identical behavior was obtained using tetrabutylammonium instead of sodium *p*-cyanophenolate. Phenolate binding appears to be very weak, possibly due to steric problems in the close approach of the phenolate to the Cu_2O_2 core in the formation of the ternary complex.

In a very recent paper,³³ binding of 2,4-di-*tert*-butylphenolate to the μ -peroxodicopper(II) complex with two didentate *N,N'*-di-*tert*-butyl-ethylenediamine (DBED) ligands at $-120 \text{ }^\circ\text{C}$ was shown to occur with isomerization to the bis- μ -oxodicopper(III) form, and evolution of this ternary intermediate yielded a 1:1 mixture of 3,5-di-*tert*-butylcatechol and 3,5-di-*tert*-butylquinone.

The reaction has the characteristics of an electrophilic aromatic substitution, with a Hammett constant $\rho = -2.2$. The fact that the ternary complex could be observed only at such extreme temperatures indicates that also in the DBED system phenolate binding is thermally very unstable. Possibly, strong immobilization of the ligand *tert*-butyl groups is necessary to stabilize phenolate binding to the Cu_2O_2 core. Formation of 1:1 catechol/quinone is also intriguing, because this ratio may suggest that the product mixture results from evolution of semiquinone radicals. In our system, addition of excess phenolate to the peroxo complex down to $-85 \text{ }^\circ\text{C}$ does not change appreciably the optical features of the peroxo complex. This could be due to the very weak interaction between the phenolate and the Cu_2O_2 complex ($K_{\text{b}} < 100 \text{ M}^{-1}$). In addition to the larger steric hindrance to the approach of phenolate to the Cu_2O_2 core in the MeL66 complex with respect to the DBED complex, phenolate binding may be intrinsically weaker to Cu^{I} centers containing tridentate (MeL66) vs didentate (DBED) donor ligands. Although we cannot exclude that a small amount of very reactive bis(μ -oxo)dicopper(III) species, rather than the μ -peroxodicopper(II) form, could be the active species also in our system, and perhaps in tyrosinase, it is interesting to note that in the monooxygenase reactions catalyzed by soluble methane monooxygenase, a dinuclear nonheme iron enzyme, the corresponding peroxodiiron(III) species is more reactive toward the substrate than the bis(μ -oxo)diiron(IV) form.³⁴

In conclusion, we have obtained for the first time the complete set of thermodynamic and kinetic parameters controlling the two steps of reversible dioxygen binding and phenol hydroxylation of a true tyrosinase model system. Unlike the enzymatic reaction,³⁵ the active site of the model system is not preorganized and this involves large activation entropy and weak phenolate binding to the active species of the monophenolase reaction. The search of model systems exhibiting a marked increase in the affinity of phenolate for the Cu_2O_2 species is essential to clarify whether the μ -peroxo \rightarrow bis- μ -oxo isomerization is a general feature accompanying the formation of the key ternary complex $[\text{Cu}_2/\text{O}_2/\text{R-Ph-O}^-]$ of the monophenolase reaction.

Supporting Information Available: Series of UV–Vis spectra recorded during deoxygenation of the $[\text{Cu}_2(\text{MeL66})\text{O}_2]^{2+}$ complex at low temperature (PDF). This material is available free of charge via the Internet at <http://pubs.acs.org>.

Acknowledgment. This work was supported by funds from a PRIN project of the Italian MIUR. The CIRCMSB is gratefully acknowledged for a fellowship to A. G.

JA0544298

(33) Mirica, L. M.; Vance, M.; Rudd, D. J.; Hedman, B.; Hodgson, K. O.; Solomon, E. I.; Stack, T. D. P. *Science* **2005**, *308*, 1890–1892.

(34) Beauvais, L. G.; Lippard, S. J. *J. Am. Chem. Soc.* **2005**, *127*, 7370–7378.

(35) Granata, A.; Monzani, E.; Bubacco, L.; Casella, L. *Chem.–Eur. J.* in press.